JOURNAL OF PROPULSION AND POWER
Vol. 17, No. 3, May–June 2001

Propulsive Performance of Hypersonic Oblique Detonation Wave and Shock-Induced Combustion Ramjets

J. P. Sislian* and H. Schirmer†
University of Toronto Institute for Aerospace Studies, Toronto, Ontario M3H 5T6, Canada
R. Dudebout‡
Honeywell Engines, Phoenix, Arizona 85072
and
J. Schumacher§
University of Toronto Institute for Aerospace Studies, Toronto, Ontario M3H 5T6, Canada

A comparative study is presented of the propulsive characteristics of hypersonic detonation wave and shock-induced combustion ramjets. The same ramjet design methodology is used to assess the propulsive performance of both types of ramjets. The lower–upper symmetric Gauss–Seidel scheme combined with a symmetric shock-capturing total variation diminishing scheme are used to solve the Euler equations describing the two-dimensional hydrogen/air combustible flowfield with nonequilibrium chemical reactions including 13 species (H_2, O_2, H, O, OH, H_2O, HO_2, H_2O_2, N, NO, HNO, N_2, and NO_2). Results obtained for flight Mach numbers $12 \leq M_\infty \leq 16$ and for a flight dynamic pressure of 67,032 Pa (1400 psf) show that combustor entrance temperatures T_{ce} (or inlet compression ratios) substantially lower than the near ignition values of hydrogen/air mixture, adopted for the generation of a near Chapman–Jouguet oblique detonation wave in the combustor, entail significant performance augmentation. For the considered range of flight Mach numbers and value of flight dynamic pressure, the thrust of a shock-induced combustion ramjet is maximum for $650 \leq T_{ce} \leq 700$ K, and at this point the combustion is entirely shock induced. The thrust generation can be enhanced by more than 10% and the fuel specific impulses improved by more than one-third over their magnitudes corresponding to maximum thrust detonation wave ramjets.

Introduction

DETONATION wave and, more generally, shock-induced combustion ramjets, or shcramjets, represent an alternative to scramjets as propulsion devices for hypervelocity vehicles. Although a substantial research effort is required for the technical implementation of this mode of hypersonic propulsion, the potential performance benefits make the effort worthwhile. An overview of past and recent research in this area has been presented, among others, in Ref. 1, where mention is made of the few attempts at predicting the propulsive characteristics of such ramjets. These predictions are based on different engine cycle assumptions or ramjet models, but they all employ an oblique detonation wave as a means of heat addition to the hypervelocity flow (see, for example, Refs. 1–9). However, results obtained in Ref. 10 show that an increase in performance parameters occurs when the combustion process is entirely shock induced rather than detonative. In Ref. 10, the considered ramjet model employed an external compression inlet with three equal strength shocks. The temperature immediately behind the third shock, at its point of inception at the cowl tip, was prescribed (Fig. 1a) effectively controlling the amount of compression in the inlet, as the accelerating vehicle climbed in a constant dynamic pressure trajectory. As the vehicle proceeded through flight Mach numbers ~14–17, the combustion process gradually changed from a predominantly detonative mode to fully shock-induced mode (Fig. 1a[10]), with an attendant increase in performance parameters within that flight Mach number range (Figs. 1b and 1c). It is of interest to explore the significance of such performance gains.

Therefore, the objective of the present investigation is to perform a meaningful comparison of the propulsive performance characteristics of detonation wave and shock-induced combustion ramjets. A brief description of the governing equations and the numerical solution employed, as well as of the methodology used to perform the comparative study is given in the next section. The findings of the study are presented next, followed by concluding remarks on the obtained results.

Numerical and Shcramjet Design Methodology

The numerical simulation of the shcramjet flowfield and its design methodology for the present comparative study closely follow the approach adopted in Ref. 1 and will be given briefly for completeness.

The two-dimensional shcramjet flowfield is described by the Euler equations for a reacting, multispecies gas in chemical nonequilibrium in curvilinear coordinates and conservative form.[1] The hydrogen/air combustion chemistry model employed is that suggested by Jachimowsky.[11] It consists of 33 reactions between 13 species (H_2, O_2, H, O, OH, H_2O, HO_2, H_2O_2, N, NO, HNO, N_2, NO_2). The numerical method employed is a fully implicit, fully coupled, Newton-iteration, total variation diminishing (TVD) scheme for solving nonequilibrium, chemically reacting flows at steady state. It combines the lower–upper symmetric Gauss–Seidel (LUSGS) method developed by Yoon and Jameson[12] and a TVD scheme developed by Yee.[13] The numerical scheme used has been validated by comparison with analytical results where available and experimental superdetonative exothermic blunt-body flows investigated by Lehr[14] (also see Ref. 1). A grid convergence study on a double-wedge planar inlet geometry for an oncoming Mach 14 perfect gas flow, with comparison of the numerical results to analytical solutions, showed the error in predicting lift and drag of the inlet to be

Received 3 December 1999; revision received 5 June 2000; accepted for publication 25 August 2000. Copyright © 2000 by the American Institute of Aeronautics and Astronautics, Inc. All rights reserved.

*Professor, Department of Aerospace Science and Engineering. Associate Fellow AIAA.
†Graduate Student, Department of Aerospace Science and Engineering.
‡Senior Engineer, Combustion and Emissions Department.
§Graduate Student, Department of Aerospace Science and Engineering; currently Senior Engineer at Honeywell Engines, Phoenix, Arizona 85072. Student Member AIAA.

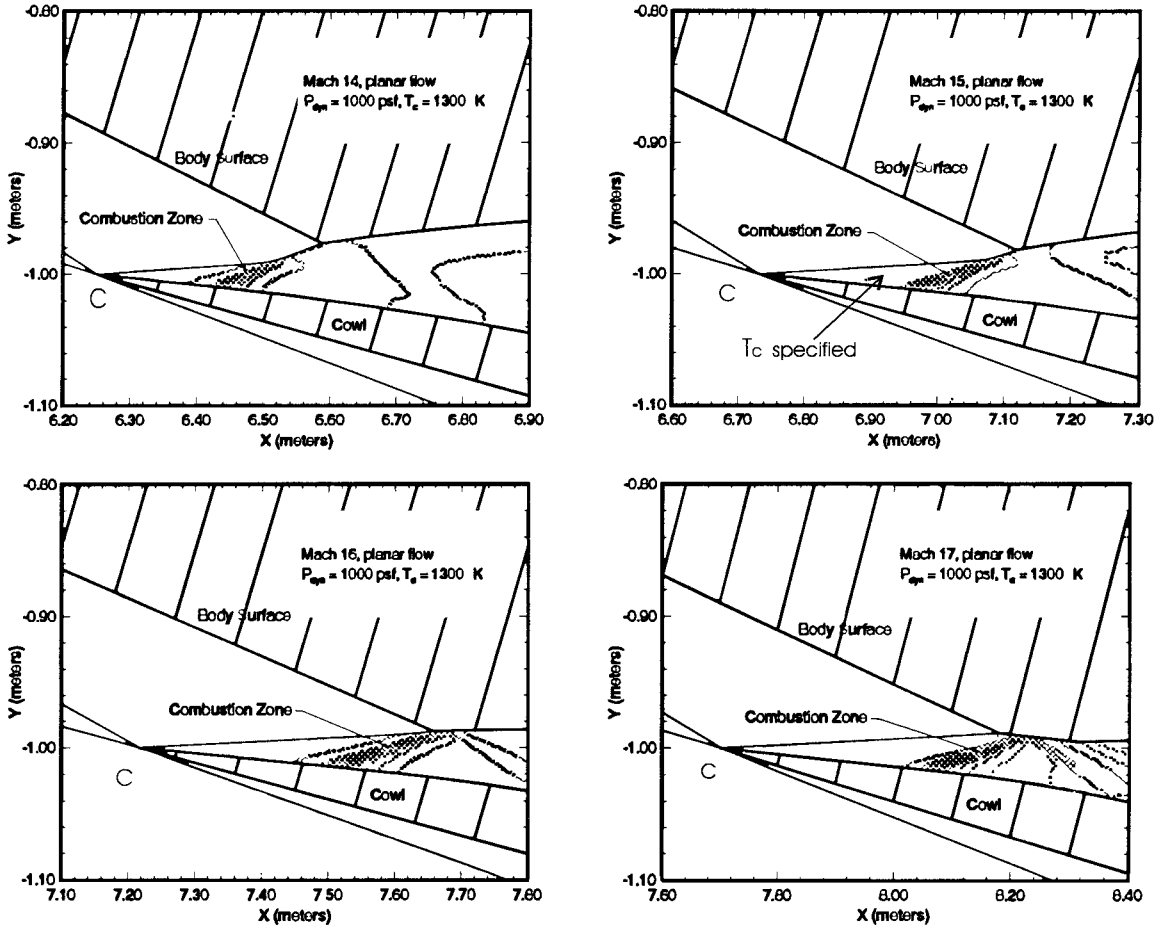

a) Evolution of the shock-induced combustion process in the $14 \leq M \leq 17$ range

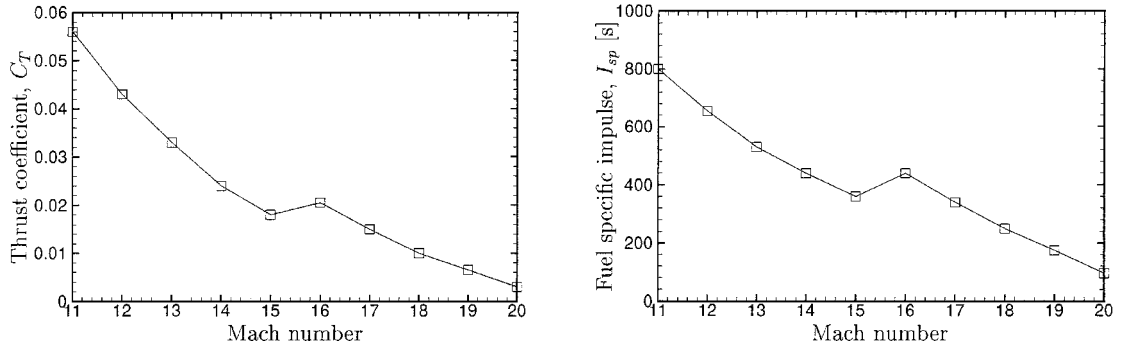

b) Thrust coefficient variation

c) Fuel specific impulse variation

Fig. 1 Combustor flowfields and corresponding propulsive characteristic variations for $14 \leq M_\infty \leq 17$, $T_{ce} = 1300$ K, and $P_{dyn} = 1000$ psf (Ref. 1).

less than 1%. Also, the numerical scheme was able to predict the splitting of the bow shock and flame front occurring in the superdetonative exothermic blunt-body flow considered by Lehr,[14] although the radial distance of the shock at the exit plane of the computational domain was about 13% overpredicted compared to Lehr's experimental data.

An external compression, planar ramjet is considered with two equal-strength shocks, which at the design flight condition, intersect at the cowl lip C (Fig. 2). It is assumed that fuel (hydrogen) is injected in the forebody/inlet flow parallel to the oncoming airflow and that a homogeneous fuel/air mixture results at the combustor entrance, DC. To simulate this, the portion of the oncoming flow above the cowl tip labeled inner flow is assumed to be a homogeneous fuel/air mixture at an equivalence ratio of 1. The portion of the flow below the leading edge of the cowl is the outer flow, composed solely of air. It is assumed that the temperature, pressure, and velocity are identical for the inner and outer flows, but their composition and, hence, densities and Mach number differ. Whereas in Ref. 1 the temperature at the end of the compression process or at the combustor entrance, DC, was set at 900 K to ensure that an oblique detonation wave is formed in the combustor, an additional degree of freedom is introduced in the present study, namely, the amount of compression in the inlet characterized by the inlet exit temperature at DC, or the combustor entrance temperature T_{ce} is successively decreased: $T_{ce} = 900$, 800, 700, 650, and 600 K for given flight dynamic pressure and Mach number. These requirements uniquely determine the planar inlet surface geometry. The inlet flowfield is solved iteratively using the nonreacting version of the Euler code. The dotted line DC represents the exit plane of the inlet and the location where the flow variables are extracted and used as inflow to the combustion system.

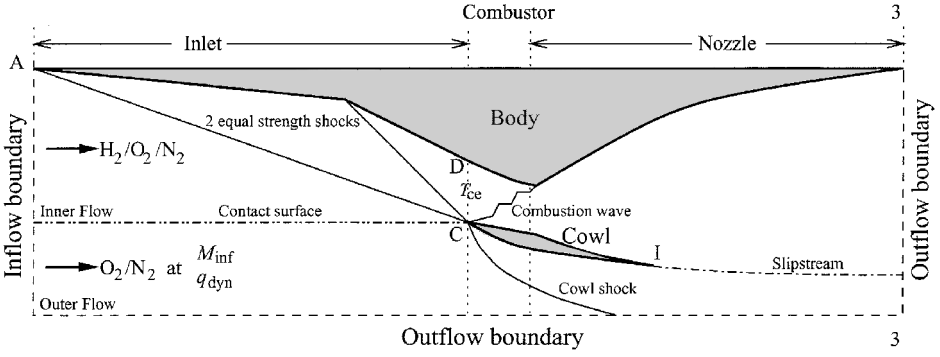

Fig. 2 Schematic of the shcramjet flowfield.

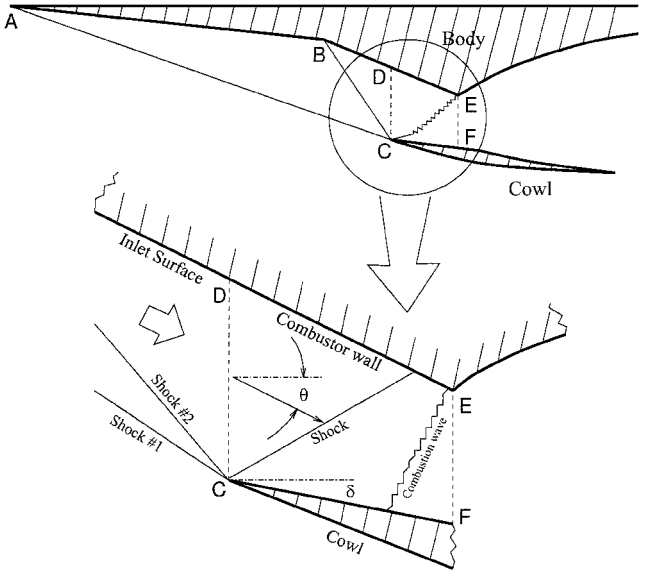

Fig. 3 Combustor design configuration.

The flowfield of the combustible mixture from the inlet is ignited in the combustor via a shock generated by the inner cowl surface CF (Fig. 3), which makes an angle δ measured from the direction of the incoming flow. For given combustor entrance conditions and depending on the magnitude of the angle δ, the ensuing combustion can be a detonation wave[1] or a shock-induced combustion (Fig. 3). The net flow deflection in the combustor is $\theta - \delta$, and point E is the location where the combustor upper (body) wall intersects the combustion wave or the detonation wave. The design criterion for determining the angle δ is minimum entropy increase throughout the combustor. In the case when a detonation wave is formed, this criterion leads to a near Chapman–Jouguet detonation.[1] To circumvent the task of finding a minimum entropy condition for all combustion regimes encountered in this study, it is assumed that low entropy production in the combustor will ultimately result in maximum thrust. Consequently, the design criterion for the choice of the cowl angle δ is maximum net thrust. Hence, the combustor and nozzle flowfields become interdependent, and proper combustor design requires the a priori knowledge of the entire flowfield. The Euler equations with the LUSGS scheme is used to solve the combustor flowfield on a domain CDEF, large enough to include the entire combustion system (Fig. 3). Data extracted along line EF provide the inflow conditions to the nozzle section. Based on these values, the nozzle is designed by the method of characteristics for rotational flow, and together with the inlet solution, the overall thrust of the shcramjet estimated. This process is repeated for different cowl angles to determine iteratively the maximum thrust configuration and the corresponding cowl angle δ_{maxth}, for given flight dynamic pressure, Mach number, and T_{ce}.

The nozzle design procedure parallels the approach given in Ref. 15. The design criteria for the nozzle are that the flow be expanded to a specific static pressure and be parallel to the freestream direction at the exit plane. The flow in the nozzle is assumed to be chemically frozen at the combustor outflow conditions. A false-wall technique is used to determine the nozzle wall contours by the method of characteristics for rotational flow. The obtained long nozzle walls are then cut off to provide 95% of the maximum thrust (to reduce frictional drag). The outer (bottom) surface of the cowl is designed by prescribing a polynomial matching the coordinates of the cowl lip and trailing edge of the cowl inner surface. At the leading edge, the cowl inclusion angle is prescribed to be 5 deg, and the trailing edge is set to be parallel to the flow. The pressures across the interface formed at point I (Fig. 2) between the propulsion streamtube and the outer flow are approximately matched to avoid the creation of a shock propagating into the nozzle flow.

Thus, the integrated shcramjet model is obtained by assembling all surfaces generated for each component of the engine, and the entire shcramjet flowfield, from tip to tail, is determined by using the numerical method for the Euler equations for nonequilibrium reacting flow of H_2/air mixtures described earlier. To ascertain the validity of the maximum thrust configuration, the shcramjet flowfields corresponding to $\delta_{maxth} + 1$ deg and $\delta_{maxth} - 1$ deg were also solved by the numerical method for the Mach 14 case.

Flowfield Analysis and Propulsive Characteristics

Computations were performed for a flight dynamic pressure of 67,032 Pa (1400 psf) and for flight Mach numbers (based on the outer flow) of $M_\infty = 12$, 14, and 16. For any given flight Mach number, the combustor entrance temperature was varied: $T_{ce} = 900$, 800, 700, 650, and 600 K.

Figure 4 shows temperature contours in the combustor section including the combustor entrance and nozzle inflow regions for $T_{ce} = 900$, 700, 650, and 600 K. In Figs. 4b–4d, the combustion is entirely shock induced with significant ignition delays. Note, however, that the combustor length (determined by the induction distance) does not noticeably increase as T_{ce} is decreased below 700 K.

The overall net thrust of the shcramjet is calculated by integrating the pressure over all wetted surfaces including the cowl outer (bottom) surface. Figure 5 shows the net thrust as a function of T_{ce} for the three flight Mach numbers considered. It can be seen that, for any given flight Mach number, the net thrust reaches a maximum for a particular value $T_{ce,maxth}$. At $M_\infty = 12$ the shcramjet produces its maximum thrust for $T_{ce,maxth} = 650$ K or, correspondingly, for a compression ratio $\Pi_c \approx 20$. Approximately the same $T_{ce,maxth}$ is optimal for $M_\infty = 14$, whereas for $M_\infty = 16$, the maximum net thrust is reached when $T_{ce,maxth} \approx 700$ K or $\Pi_c \approx 21$. Figure 5 shows a general trend: As the flight Mach number increases, the maximum thrust tends to occur at higher T_{ce} values. Compared to the $T_{ce} = 900$ K case of a maximum thrust near Chapman–Jouguet detonation wave ramjet considered in Ref. 1, the total gain in net maximum thrust of shock-induced combustion ramjets amounts to ~9% at $M_\infty = 12$, ~12% at $M_\infty = 14$, and ~20% at $M_\infty = 16$ (see Fig. 5).

The thrust contributions of various engine components, at $M_\infty = 14$, of a near Chapman–Jouguet (maximum thrust) detonation wave

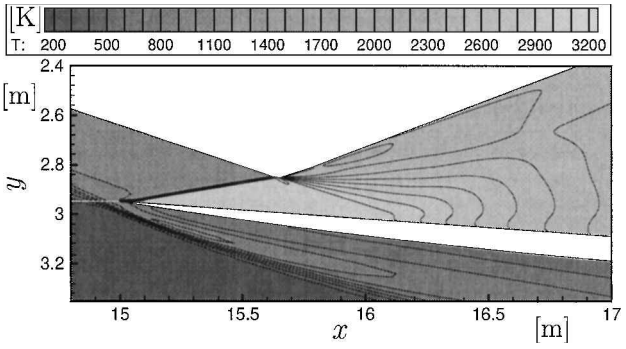

a) Combustor entrance temperature $T_{ce} = 900$ K, cowl angle $\delta = 4$ deg, net deflection angle $\theta - \delta = 14.5$ deg; predominantly detonation wave configuration

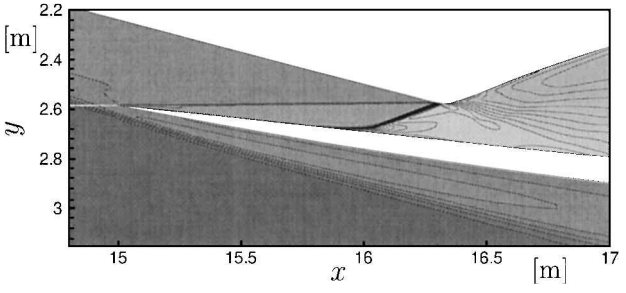

b) Combustor entrance temperature $T_{ce} = 700$ K, $\delta = 6$ deg, and $\theta - \delta = 8.5$ deg; shock-induced combustion

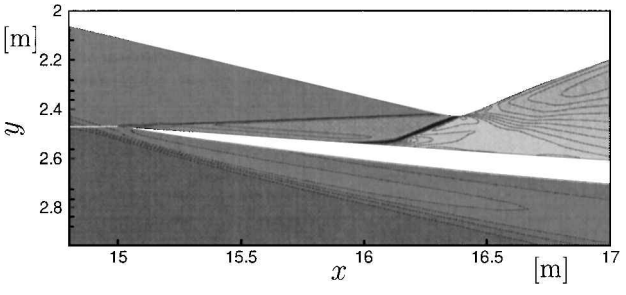

c) Combustor entrance temperature $T_{ce} = 650$ K, $\delta = 4$ deg, and $\theta - \delta = 9.4$ deg; maximum thrust shock-induced combustion configuration

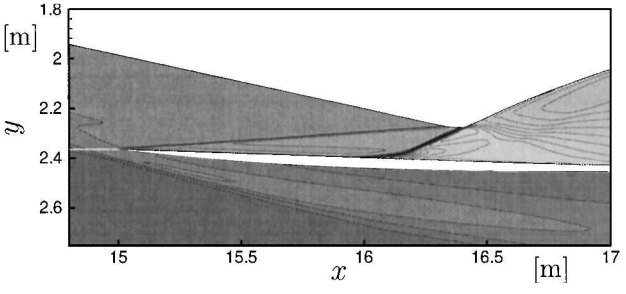

d) Combustor entrance temperature $T_{ce} = 600$ K, $\delta = 2$ deg, and $\theta - \delta = 10.3$ deg; shock-induced combustion configuration

Fig. 4 Temperature contours in the combustor section and the nozzle inflow: $M_\infty = 14$ and $P_{dyn} = 67{,}032$ Pa (1400 psf).

ramjet ($T_{ce} = 900$ K) are compared to those of a maximum thrust shock-induced combustion ramjet ($T_{ce,maxth} = 650$ K) in Fig. 6. It can be seen that the shcramjet mainly profits from the lower drag produced by the inlet. Lesser degree of compression results in a low-pressure level throughout the engine, which is only partially compensated by a higher heat addition in the combustor (higher H_2O production). Consequently, the pressure in the nozzle remains below the values corresponding to the $T_{ce} = 900$ K predominantly detonation wave case, and the nozzle produces less thrust. However, the advantage of decreased compression is significant, less than half

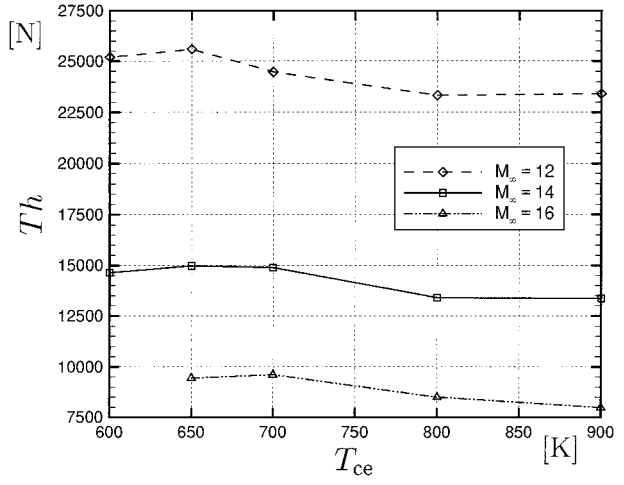

Fig. 5 Installed net thrust of the shcramjet.

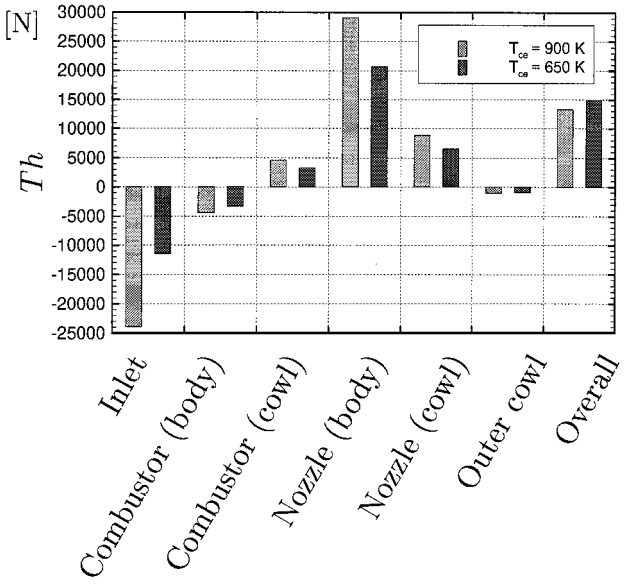

Fig. 6 Thrust contributions broken down into engine sections for the $M_\infty = 14$ case; near Chapman–Jouguet (maximum thrust) detonation wave ramjet vs maximum thrust shock-induced combustion ramjet.

the drag force is induced, and, therefore, the thrust revenues increase appreciably.

However, the impact of the combustion mode on thrust deserves further emphasis. To observe the effects of a change in the combustion mode on the magnitude of net thrust, isolated from the effects of degree of compression, three configurations are compared. The inlet compression is fixed at $T_{ce} = 700$ K and the cowl angle δ varied. From Fig. 7a, it can be observed that for $\delta = 5$ deg, the gas mixture is partially burned in a detonation wave, whereas for $\delta = 6$ and 7 deg, the combustion is entirely shock induced. Maximum thrust is produced when the cowl angle is chosen such that the combustion is entirely shock induced and the shock and combustion waves intersect simultaneously on the combustor upper wall (compare Figs. 7b and 7c, see also Fig. 5). Figure 8, which depicts the thrust contributions of each engine component for the three configurations considered, shows that the increased drag induced by the combustor upper wall cancels out with the enhanced thrust generated by the combustor cowl surface, so that changes in nozzle thrust dominate the overall thrust production. Although the outer surface of the cowl causes more drag at greater δ angles, the overall nozzle thrust gain prevails. When the cowl angle is further increased ($\delta = 7$ deg), the cowl drag penalty becomes excessive. Because the gain in nozzle thrust is marginal, it cannot overcome the cowl drag, and the overall thrust is decreased.

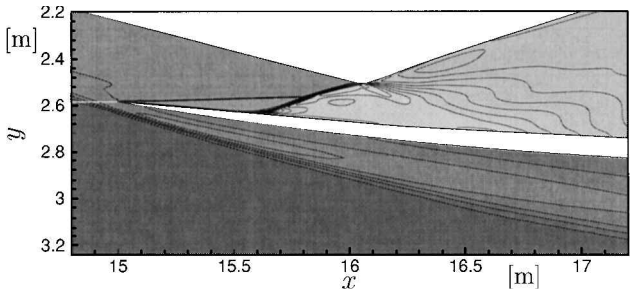

a) Combustor entrance temperature $T_{ce} = 700$ K, $\delta = 5$ deg, $\theta - \delta = 9.5$ deg, and $Th = 14{,}181$ N

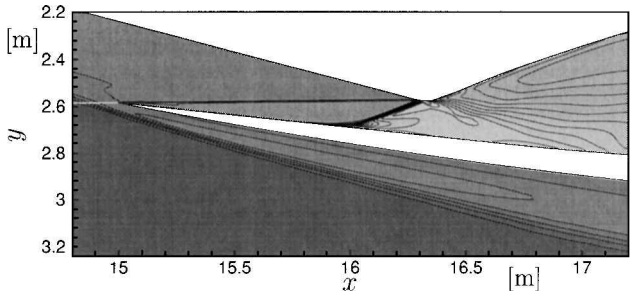

b) Combustor entrance temperature $T_{ce} = 700$ K, $\delta = 6$ deg, $\theta - \delta = 8.5$ deg, and $Th = 14{,}897$ N; maximum thrust configuration

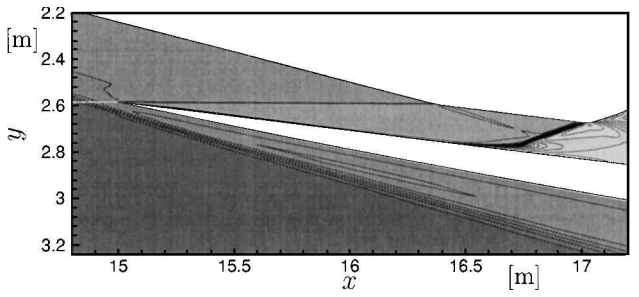

c) Combustor entrance temperature $T_{ce} = 700$ K, $\delta = 7$ deg, $\theta - \delta = 7.5$ deg, and $Th = 13{,}065$ N

Fig. 7 Temperature contours in the combustor section.

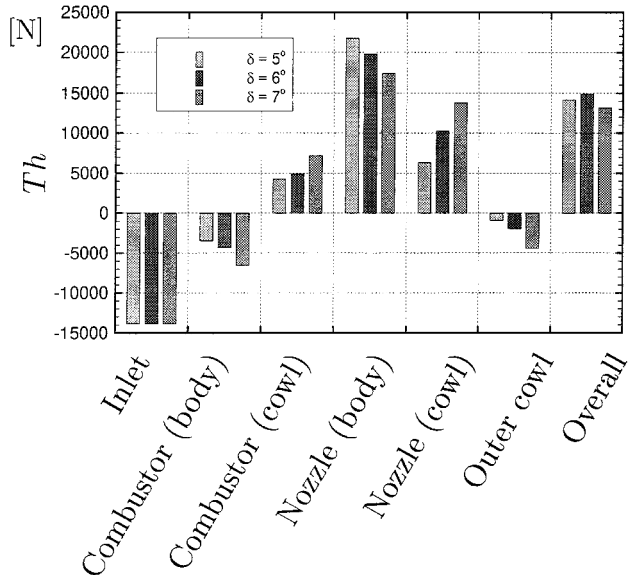

Fig. 8 Thrust contributions broken down into engine sections for the $M_\infty = 14$ and $T_{ce} = 700$ K case; variation of the cowl angle.

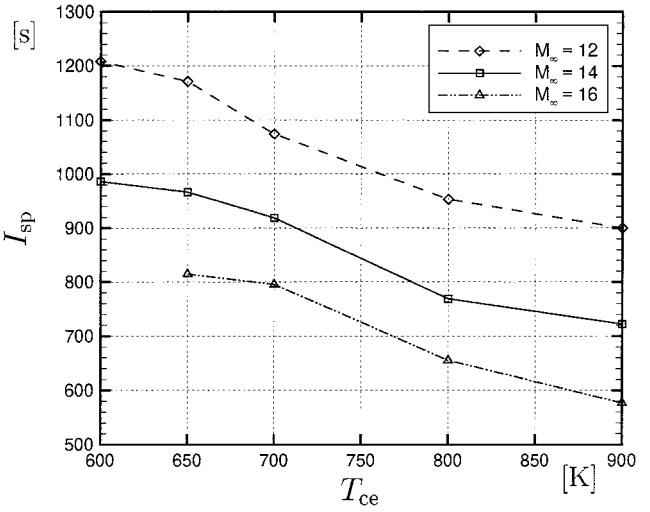

Fig. 9 Specific impulse of the shcramjet.

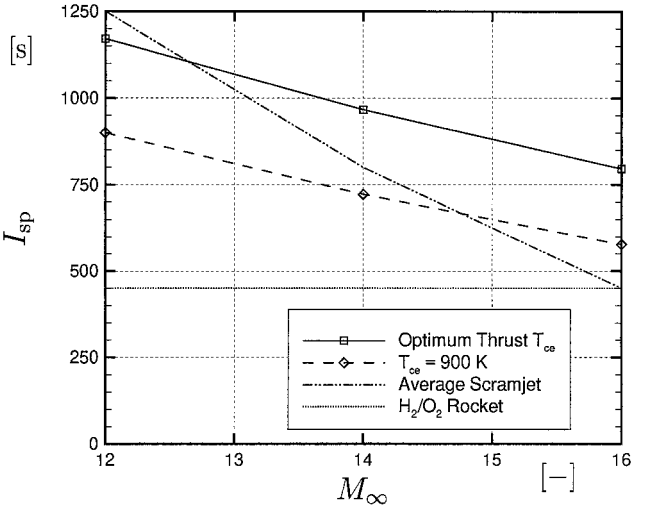

Fig. 10 Specific impulse as a function of freestream Mach number.

The variations of the fuel specific impulse, $I_f = Th/\dot{m}_f g$, for the maximum-thrust cases considered are presented in Fig. 9. This parameter increases continually with decreasing T_{ce}. The plots display the superior thrust efficiency of the shcramjet for low combustor entrance temperatures. The gain in specific impulse compared to that of a detonation wave ramjet is significant: ~30, 34, and 38% at $M_\infty = 12$, 14, and 16, respectively. Figure 10 shows the specific impulse of a predominantly detonation wave ramjet ($T_{ce} = 900$ K), a maximum-thrust, shock-induced combustion ramjet, of a generic scramjet (calculated using the hypersonic airbreathing propulsion computer program of Ref. 16 based on average or most-probable values of scramjet component efficiency estimates for approximately the same flight dynamic pressure trajectory) and of a H_2/O_2 rocket, for $12 \leq M_\infty \leq 16$. It can be seen that the shcramjet specific impulse is comparable to that of a scramjet at $M_\infty = 12$ and exceeds the scramjet values for higher Mach numbers. The shcramjet produces more than double the specific impulse of a H_2/O_2 rocket for $M_\infty = 12$–14 and maintains superior specific impulse at $M_\infty = 16$ and probably beyond.

Finally, of great practical interest is the degree of variable geometry required for ondesign shcramjet operation. Figure 11 shows that the combustor length of a shcramjet is approximately twice as large as that of a detonation wave ramjet ($T_{ce} = 900$ K), but changes little with increasing flight Mach number. Therefore, geometric variability reduces to the adjustment of the cowl angle δ and to its vertical positioning only.

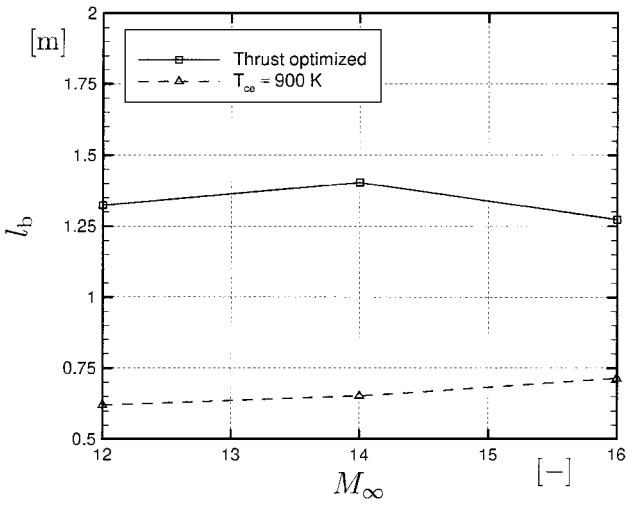

Fig. 11 Combustor length as a function of freestream Mach number.

Concluding Remarks

It has been shown that inlet outflow temperatures T_{ce} substantially lower than the near ignition values of a hydrogen/air combustible mixture entail significant performance augmentation. The thrust generation can be enhanced by more that 10% and the fuel specific impulse improved by more than one-third over its magnitude at high T_{ce}. Thrust generation has been found to reach its maximum for $650 \leq T_{ce} \leq 700$ K for the considered range of flight Mach numbers or for the corresponding pressure ratio of $\Pi_c \approx 20$. Most of the gain is due to the lower compression ratio and thus less compression work in the inlet. However, it has also been shown that the combustion must be entirely shock induced to attain maximum thrust. Lower temperatures in the inlet reduce the risk of premature ignition during the mixing process, and cooling loads are decreased. Although the combustor length doubles due to longer induction distances, it maintains an approximately constant value over the range of flight Mach numbers. Hence, geometric variability reduces to the adjustment of the cowl angle and to its vertical positioning only.

References

[1]Dudebout, R., Sislian, J. P., and Oppitz, R., "Numerical Simulation of Hypersonic Shock-Induced Combustion Ramjets," *Journal of Propulsion and Power*, Vol. 14, No. 6, 1998, pp. 869–879.

[2]Dunlap, R., Brehm, R. L., and Nicholls, J., "A Preliminary Study of the Application of Steady-State Detonation Combustion to a Reaction Engine," *Journal of Jet Propulsion*, Vol. 28, No. 6, 1958, pp. 451–456.

[3]Sargeant, W., and Gross, R. A., "A Detonation Wave Hypersonic Ramjet," TN 589, Air Force Office of Scientific Research, June 1959.

[4]Townend, L. H., "Detonation Ramjets for Hypersonic Aircraft," Royal Aircraft Establishment, Bedford, TR 70218, Nov. 1970.

[5]Morrison, R. B., "Evaluation of the Oblique Detonation Wave Ramjet," NASA CR 145358, 1978.

[6]Morrison, R. B., "Oblique Detonation Wave Ramjet," NASA, CR 159192, 1980.

[7]Ostrander, M., Hyde, J., Young, M., and Kissinger, R., "Standing Oblique Detonation Wave Engine Performance," AIAA Paper 87-2002, 1987.

[8]Ashford, S. A., and Emanuel, G., "Oblique Detonation Wave Engine Performance Prediction," *Journal of Propulsion and Power*, Vol. 12, No. 2, 1996, pp. 322–327.

[9]Sislian, J., and Atamanchuk, T., "Aerodynamic and Propulsive Performance of Hypersonic Detonation Wave Ramjets," *Proceedings of the Ninth International Symposium on Air-Breathing Engines*, AIAA, Washington, DC, 1989, pp. 1026–1035.

[10]Sislian, J., and Dudebout, R., "Hypersonic Shock-Induced Combustion Ramjet Performance Analysis," *Proceedings of the Eleventh International Symposium on Air-Breathing Engines*, AIAA, Washington, DC, 1993, pp. 413–420.

[11]Jachimowsky, C. J., "An Analytical Study of the Hydrogen-Air Reaction Mechanism with Application to Scramjet Combustion," NASA TP-2791, 1988.

[12]Yoon, S., and Jameson, A., "A Lower–Upper Symmetric Gauss–Seidel Method for the Euler and Navier–Stokes Equations," *AIAA Journal*, Vol. 26, No. 9, 1988, pp. 1025, 1026.

[13]Yee, H. C., "Upwind and Symmetric Shock-Capturing Schemes," TR TM-89464, NASA, 1987.

[14]Lehr, H. F., "Experiments on Shock-Induced Combustion," *Astronautica Acta*, Vol. 17, No. 10, 1972, pp. 589–597.

[15]Sislian, J. P., Dudebout, R., Schumacher, J., Islam, M., and Redford, T., "Incomplete Fuel/Air Mixing and Off-Design Flight Effects on Hypersonic Shock-Induced Combustion Ramjet Performance," *Journal of Propulsion and Power*, Vol. 16, No. 1, 2000, pp. 41–48.

[16]Pratt, D. T., and Heiser, W. H., *Hypersonic Airbreathing Propulsion*, AIAA Education Series, AIAA, Washington, DC, 1994, p. 587.